

A PHYSICAL MODELLING STUDY OF INCLUSION REMOVAL IN TUNDISH USING INERT GAS CURTAIN

Varadarajan Seshadri ¹
Carlos Antônio da Silva ²
Itavahn Alves da Silva ³
Ely da Silva Araújo Júnior ⁴

Abstract

The control and minimization of non-metallic inclusions content in the tundish and in the mold of a continuous casting unit is crucial for ensuring the final quality of the steel cast product. Nonmetallic inclusions of sizes smaller than 15 μm are hard to remove, as they are difficult to float. They are easily carried by the flow of steel melt into the mold and adversely affect the steel cleanliness. It is suggested that a gas curtain made of small bubbles of argon can be used to capture and remove these inclusions in the tundish, thus avoiding their transport into the mold. A 1:3 scale physical model of tundish of the continuous casting unit of ArcelorMittal plant, in Vitória, Brazil, was built to investigate the effects of gas flow, shape and positioning of the gas curtain inside the tundish, on the efficiency of removal of inclusions. The results suggest that the gas bubbling inside the tundish can be effective in inclusion removal. The efficiency is dependent upon the location of argon bubbling.

Key words: Modelling; Inclusion removal; Tundish.

1 INTRODUCTION

The tundish of the continuous casting machine performs many complex functions. It serves as reservoir, distributor of liquid steel to the strands controlling flows, especially during the transitional arrangements, promotes thermal homogeneity, thermal insulation, composition control of liquid steel enabling addition of alloying elements, prevention of reoxidation by air, coalescence, flotation and removal of non-metallic inclusions etc.

The rate of contamination of the liquid steel in the tundish can be controlled by the adoption of some important operational practices, such as slag cover, efficient sealing, protection of jet from ladle from oxidation, inhibition of vortices, complete flux covering of the surface of the metal with quick formation of a tundish slag with low contents of FeO, and MnO.

The practice of bubbling inert gas in the ladle or in tundish, prior to continuous casting,⁽¹⁻⁸⁾ improves the rates of collision and agglomeration of inclusions increasing the rate of flotation of inclusions by the colony of bubbles and formation of clusters of larger sizes. The high degree of turbulence prevailing inside the valve and the good rate

of mixing of liquid steel promote the generation of a zone of finely dispersed bubbles, providing better chances of collision coalescence and capture of non-metallic inclusions and greater ability to absorb gaseous impurities. Results from physical modelling, according to Wang, Lee and Hayes,^(7,8) indicate the existence of a zone of finely dispersed bubbles, especially when the injection of inert gas is carried out through a partially open valve because of the high state of turbulence. The results also showed that the formation of vortex favoured the formation of fine bubbles with diameters from 0.3 mm to 0.5 mm, and a uniform distribution of bubbles around the jet from the ladle, favouring the capture and removal of inclusions.

A curtain of bubbles of argon in the tundish changes the flow pattern of liquid steel stimulating the recirculating flows that favour collision, coalescence and flotation of inclusions and capture of a broad spectrum of sizes of inclusions by the train of bubbles spreading longitudinally. The rate of bubbling has to be properly controlled, because an excessive flow can cause such levels of turbulence that facilitates the emulsification of the slag coverage and exposure of the metal to the air, thus stimulating

¹Dr. Ing. Emeritus Professor, Department of Metallurgical Engineering and Materials, Federal University of Minas Gerais – UFMG, Av. Antonio Carlos, 6627, CEP 31270-901, Belo Horizonte, MG, Brazil. E-mail: seshadri@demet.ufmg.br

²PhD. Associate Professor, Department of Materials Engineering, Federal University of Ouro Preto – UFOP, Campus do Morro do Cruzeiro, Escola de Minas, Bauxita, CEP 354000-000, Ouro Preto, Minas Gerais, Brazil. E-mail: casilva@em.ufop.br

³DSc. Associate Professor, Department of Materials Engineering, Federal University of Ouro Preto – UFOP, Campus do Morro do Cruzeiro, Escola de Minas, Bauxita, CEP 354000-000, Ouro Preto, Minas Gerais, Brazil. E-mail: itavahn@em.ufop.br

⁴MSc, Avenida Rita Maria Ferreira, 855, apto 504, Prédio Estados Unidos, Bairro Comercial, CEP 275 10-060, Resende, RJ, Brazil. E-mail: elyjuniorf8@yahoo.com.br

the reoxidation of the metal bath, and the absorption of nitrogen. If all these factors are taken in consideration inert gas injection can be used as a means of promoting steel cleanliness.

This work deals with the evaluation of the effect on the efficiency of flotation of inclusions inside a tundish as influenced by variables such as inert gas injection flow rate, porous plug superficial area and position for injection and other variables, simulating the conditions of tundish of ArcelorMittal Tubarão #2 continuous casting unit. With this objective, a physical model was constructed and operated in the laboratory, considering the tundish geometry as well as operational parameters from the industrial installation.

2 PHYSICAL MODELLING OF RISE OF INCLUSIONS IN THE TUNDISH

For the range of sizes of inclusions in the tundish, one can assume that they float inside the steel with a terminal velocity that can be evaluated by Stokes law. Accordingly, the terminal velocity of particles in the model (m) and prototype (p) can be given as (Equations 1 and 2):

$$u_{p,m}^m = \frac{2r_{p,(m)}^2 g (\rho_L^m - \rho_p^m)}{9\eta_L^m} \quad (1)$$

and

$$u_{p,p}^p = \frac{2r_{p,(p)}^2 g (\rho_L^p - \rho_p^p)}{9\eta_L^p} \quad (2)$$

Here, u_p stands for inclusion velocity, r_p for radius of the inclusion, g for gravity acceleration, ρ_L and ρ_p for liquid and inclusion densities, respectively, and η stands for liquid viscosity.

Also, using similarity criteria of Froude, the liquid velocities, u_L , are related by (Equation 3),

$$\frac{u_L^m}{u_L^p} = \sqrt{\lambda} \quad (3)$$

where λ is the scale factor. For kinematic similarity for the distribution of velocities and the trajectories of particles in the model and the prototype the following criteria for the model and prototype can be applied (Equation 4):

$$\left(\frac{u_L}{u_p} \right)_m = \left(\frac{u_L}{u_p} \right)_p \quad (4)$$

This is the required condition for achieving similar trajectories of particles in the model as compared with the prototype. Then, applying Froude criteria and considering terminal velocities for model (m) and prototype (p) as given before (Equations 5 and 6):

$$\frac{u_{p,m}^m}{u_{p,p}^p} = \frac{1}{\sqrt{\lambda}} \quad (5)$$

and

$$\frac{u_{p,m}^m}{u_{p,p}^p} = \frac{r_{p,(m)}^2 (\Delta\rho)_m \eta_L^p}{r_{p,(p)}^2 (\Delta\rho)_p \eta_L^m} = \frac{1}{\sqrt{\lambda}} \quad (6)$$

If the kinematic viscosity of liquids in model and prototype (water and steel) are considered equal one can write (Equations 7 and 8):

$$\frac{r_{p,(m)}}{r_{p,(p)}} = \frac{1}{\lambda^{1/4}} \left[\frac{\left(\frac{1 - \rho_p}{\rho_L} \right)_p v_L^m}{\left(\frac{1 - \rho_p}{\rho_L} \right)_m v_L^p} \right]^{1/2} \quad (7)$$

or

$$\frac{r_{p,(m)}}{r_{p,(p)}} = \sqrt[4]{ \frac{\left(\frac{1 - \rho_p}{\rho_L} \right)_p \lambda^{-1/4}}{\left(\frac{1 - \rho_p}{\rho_L} \right)_m} } \quad (8)$$

Flow of argon and air in the prototype and model can be related on the basis of modified Froude number (Fr') as a criterion of similarity. If ρ_g stands for gas density, u_g for gas superficial velocity and H for liquid level inside the tundish then (Equation 9),

$$Fr' = \left[\frac{\rho_g u_g^2}{\rho_L g H} \right]_m = \left[\frac{\rho_g u_g^2}{\rho_L g H} \right]_p \quad (9)$$

The superficial gas velocity at the exit of each orifice for bubbling of argon is given by (Equation 10):

$$u_g = \frac{4 Q}{\pi d_o^2 N_o} \quad (10)$$

where: Q is the gas flow rate, d_o , the size of each orifice and N_o the number of orifices. Using this in the modified Froude criteria (Equation 11):

$$\left[\frac{16\rho_g Q^2}{\rho_L g \pi^2 H N_o^2 d_o^4} \right]_m = \left[\frac{16\rho_g Q^2}{\rho_L g \pi^2 H N_o^2 d_o^4} \right]_p \quad (11)$$

Finally, assuming that the number of orifices are same for the injection of gas in the model and the prototype (Equations 12 and 13):

$$\left[\frac{\rho_g Q^2}{\rho_L H N_o^2 d_o^4} \right]_m = \left[\frac{\rho_g Q^2}{\rho_L H N_o^2 d_o^4} \right]_p \quad (12)$$

Hence,

$$\left(\frac{Q_m}{Q_p}\right)^2 = \left(\frac{\rho_g}{\rho_L}\right)_p \left(\frac{\rho_L}{\rho_g}\right)_m \left(\frac{d_{O_2}^m}{d_{O_2}^p}\right)^4 \left(\frac{H_m}{H_p}\right) \quad (13)$$

Considering geometric similarity between the orifices of model and prototype for injection of gas, one gets (Equations 14 and 15):

$$\left(\frac{Q_m}{Q_p}\right)^2 = \left(\frac{\rho_g}{\rho_L}\right)_p \left(\frac{\rho_L}{\rho_g}\right)_m \lambda^5 \quad (14)$$

or

$$Q_m = \sqrt{\left(\frac{\rho_g}{\rho_L}\right)_p \left(\frac{\rho_L}{\rho_g}\right)_m} \lambda^{5/2} Q_p \quad (15)$$

These are the relations that result from the similarity criteria. These have to be taken into consideration, for determining the parameters of the model using the parameters of the prototype for the construction and operation of the physical model.

3 EXPERIMENTAL SET UP AND METHODOLOGY

A 1:3 scale physical model of tundish of Arcelor-Mittal Tubarão #2 continuous casting machine was built and operated under conditions determined on the basis of similarity criteria. The model was built in acrylic, consisting of different geometrical aspects of the prototype such as inhibition of turbulence and others such as the Yield Enhancement System.

As can be seen from Figure 1, the tundish model feeds 2 strands (or 2 molds). Inclusion flotation efficiency can be assessed by comparing the results obtained for the two strands. One of them is operated without gas injection and air is injected in the other one (simulating inert gas in the prototype). The industrial tundish has a working volume for 60 tons with a casting capacity of 9 tons/minute. On the basis of similarity criteria discussed in the previous section, Froude number can be used to assess the water flow rate and other parameters on the basis of similarity criteria. Plastic particles (50 to 100 μm and 100 to 200 μm ; density of 0.97 g/cm^3) were injected at the ladle-tundish nozzle to simulate the pulse of inclusions. These size ranges of plastic particles were arrived at from similarity criteria with inclusions in steel melt, assuming an average inclusion density of 4000 kg/m^3 and steel density of 7000 kg/m^3 . Since the scale factor λ is 1/3, the ratio between actual inclusion size and chosen plastic particle size range yields $r_m/r_p \approx 6$ in accordance with the similarity criteria equation for the same given in the previous section. Hence these two ranges simulate inclusions from 10 μm to 15 μm and from 15 μm to 30 μm in the actual tundish of the continuous casting machine. In the experiments, a given volume of a particle – water – alcohol pulp was pumped using a peristaltic pump. Metallic sieves with opening of 63 μm (0.063 mm), installed at the two tundish outlets with SEN (Submerged Entry Nozzles), enable the non-floated particles to be captured and weighed for comparison purposes. Thus in a typical experiment of defined process parameters, the weight of particles, captured at the two strands and that of particles skimmed on the top of the liquid, can be evaluated.

To simulate the injection of inert gas through the bottom of the tundish, a system of injection of compressed

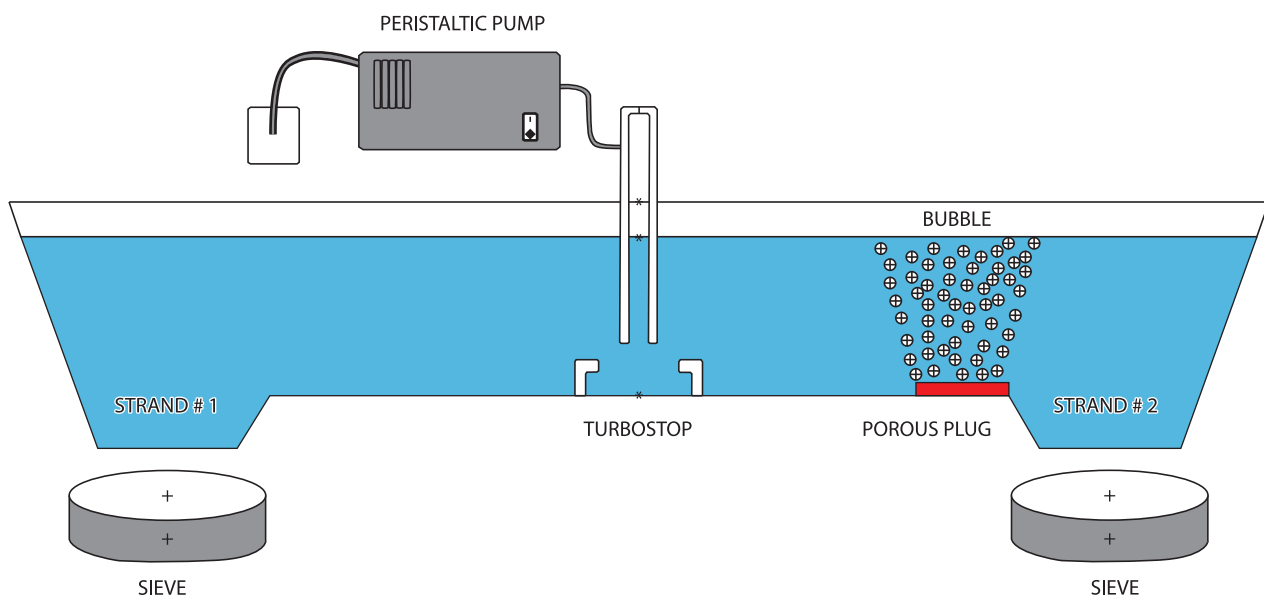


Figure 1. Schematics of the assembly of the tundish model with the peristaltic pump system, gas injection and positioning of the screens.

air with a mass flow meter was provided. A rectangular piece of porous silica-alumina or any other ceramic base material was installed on one side of the strand #2. The two refractory materials used can generate different bubble sizes depending on their grain texture, pore sizes and wettability.

4 RESULTS AND DISCUSSION

Two slightly different experimental set-ups have been provided. The first one is schematically shown in Figure 1. Ceramic materials such as silica-alumina refractory, basic refractory, all of rectangular shape were used to fabricate porous pieces. The width (W) was kept constant whereas the length (L) can vary. The plug location was defined by measuring the distance between the middle of each one to the ceramic nozzle (Figure 2)

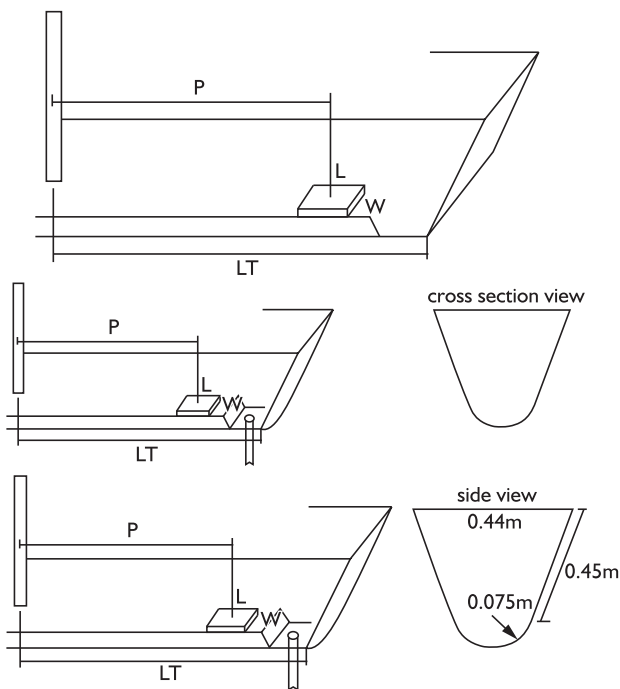


Figure 2. Porous piece location, dimensions and side view of tundish model: P = 0.42 m and 0.65 m; W = 0.12 m; L = 0.12 m and 0.195 m; LT = 1.40 m. LT is the length of the tundish; L is the length of the porous piece; W is the width of porous piece; P is the distance between nozzle and the middle of the porous piece; Internal diameter of SEN = 0.035 m.

Figure 3 gives the effect of porous piece size, its location in relation to the valve and flow of injected air. It can be observed that, in the case of larger porous piece, the percentage of particles recovered in the sieve located underneath the tundish outlet #2 is relatively lower (the porous plug responsible for additional inclusion flotation is installed at this side of the tundish) and the injection of

gas in general, promotes better particle removal. It is also noticed that with the closeness of the porous plug to the ceramic nozzle, the extent of inclusion removal becomes better. However this effect is smaller when a larger porous piece is employed. These results may be due to the curtain of air that acts as a filter for particles, and its effect on the installation of an upward flow, which is more efficient as it is induced near the entrance of the metal. In this case, the larger piece could be forming a more intense upward flow, diminishing the effect of the position.

In all cases, it can be verified that the flow of air has a negligible effect on results. This suggests the existence of a critical flow rate. Above this critical value, this variable no longer influences the removal of inclusions.

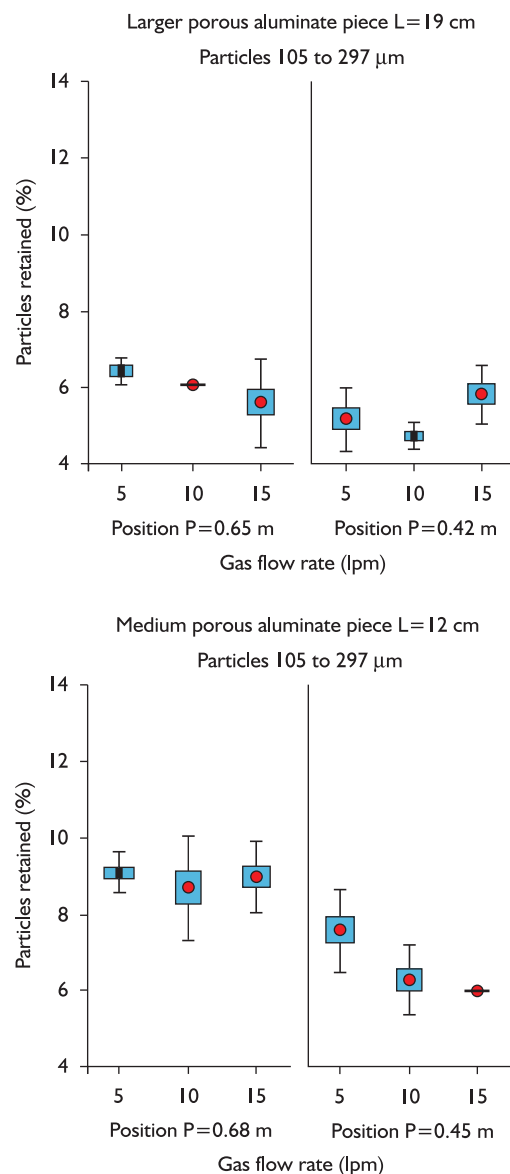


Figure 3. Effect of the size of the porous silicon-alumina plug, its position and air flow rate on the % of particles retained at the side with gas injection.

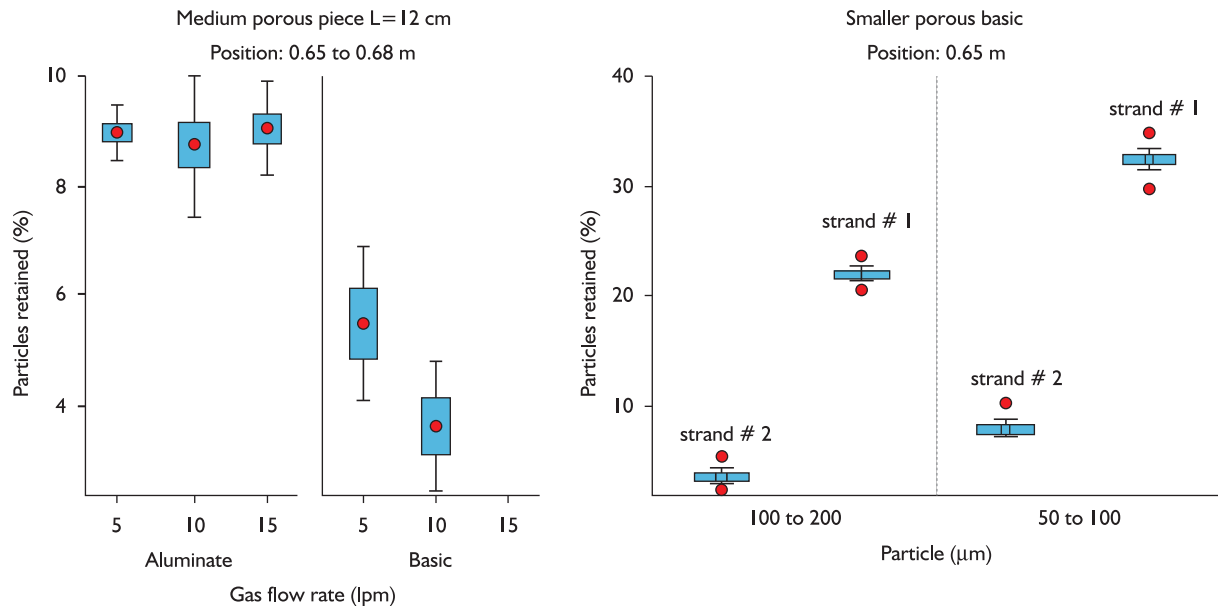


Figure 4. Percentage of particles collected at the sieve located at the air injection side (all trials), relative to the total amount injected.

The effect of the type of porous material is given in Figure 4. The plug made of basic refractory presents superior performance as compared to silicon-alumina material. This may be due to greater homogeneity of pores in the case of basic refractory, which promotes the formation of more uniform plume made of finer bubbles. Figure 4 suggests that this technique would be more efficient in the case of larger particles as shown by a comparison between strand #2 and strand #1. However, Inclusions with smaller sizes are more likely to be dragged into the mold.

The second experimental set-up employed a ceramic piece around the tundish outlet. This arrangement should be more convenient, since there are safety concerns in respect of the tubes for argon injection inserted in the refractory. A shaft made of bubbles arising around the strand outlet may provide a filter or barrier to the entry of inclusions.

As a matter of fact bubbling inert gas around the strand (Figure 5) seems to be effective in inclusion removal. However, it was less effective in comparison with the previously investigated arrangement because of the fact that part of the gas bubbles in the vicinity of the strand was probably dragged into the mold. Increased inert gas flow rate resulted in greater efficiency of capture and removal of inclusions, because of the presence of a larger population of bubbles in the vicinity of gas curtain. However this can give rise to more bubbles dragged into the mold.

According to Thomas and Bai,⁽⁵⁾ argon gas flow rate should be about 5 NL/min to avoid clogging since the film of gas formed along the wall of the valve can inhibit the contact between the wall and the inclusions. Also the injected gas may facilitate the capture and flotation of

inclusions in the upper region of the mold and also reduce the aspiration of air. Hence, some drag of bubbles into the mould would not be detrimental.

In order to assess the influence of gas injection on the macroscopic flow of liquid inside the tundish, a series of DTR (distribution of residence time) curves have been determined using the pulse technique (in this case the pulse injection of a KCl solution at the tundish entry followed by conductivity measurements at the tundish outlets). All the combinations of porous piece size, position and gas flow rate have been tested. It is generally accepted that an increased fraction of piston flow leads to a higher probability of inclusion removal. The piston flow fraction is usually defined as the ratio between the Minimum Residence Time, T_{min} , and the Nominal Residence Time of liquid inside the tundish (τ). Thus if V_T stands for the internal volume of the tundish and Q for the volumetric liquid flow rate (Equation 16):

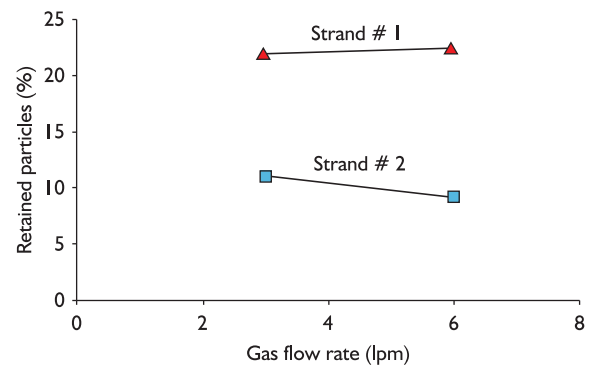


Figure 5. Effect of blowing air around the tundish outlet #2 (basic refractory).

$$\text{Fraction of piston flow} = \frac{T_{\min}}{\tau} = \frac{T_{\min} Q}{V_T} \quad (16)$$

V_T and Q are kept constant throughout these experiments and hence T_{\min} would be the direct measurement of the ability of the tundish in respect of inclusion flotation. However, gas injection seems (Figure 6) to decrease the fraction of piston flow. This effect is stronger on the gas injection side. Thus inclusion removal by gas injection cannot be attributed to a more favorable macroscopic flow.

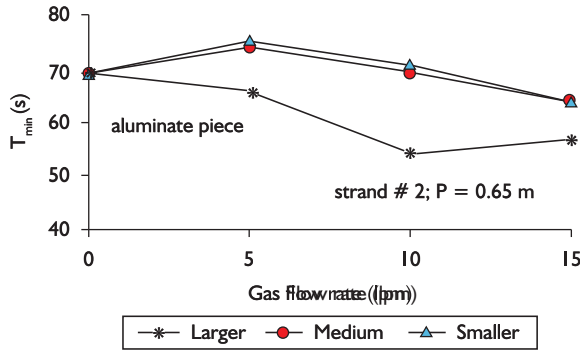


Figure 6. Fraction of piston flow at gas injection side (as measured by the minimum residence time) as a function of gas flow rate.

Some of these results can be anticipated by using a model reported by Rogler.⁽³⁾ According to this model, if the inclusion diameter is d (plastic particles of $20 \times 10^{-6} m$ or $40 \times 10^{-6} m$) and the bubble diameter is d_b (around $1 \times 10^{-3} m$, using photographic evidence) their ascension velocities can be estimated by using Stokes law (Equations 17 and 18),

$$u = \frac{d^2}{18 \eta} g(\rho_L - \rho) \quad (17)$$

and

$$u_b = \frac{d_b^2}{18 \eta} g(\rho_L - \rho_b) \quad (18)$$

Here η and ρ_L are the viscosity and density of the liquid (water, $1 \times 10^{-3} Pa.s$ and $1000 kg.m^{-3}$, respectively); g is the acceleration due to gravity, ρ and ρ_b are the particle and gas densities ($950 kg.m^{-3}$ and $1 kg.m^{-3}$) respectively. Reynolds number for the ascending bubble is given by $Re = d_b u_b \rho_L / \eta$, and from its value the following parameters can be evaluated (Equations 19-22):

$$X = \frac{3}{2} + \frac{9 Re}{32 + 9.888 Re^{0.694}} \quad (19)$$

and

$$Y = \frac{3 Re}{8 + 1.736 Re^{0.694}} \quad (20)$$

$$C = \frac{u}{u_b} \left(\frac{d_b}{d} \right)^2 \quad (21)$$

and

$$D = \frac{\sqrt{(X+C)^2 + 3Y^2} - (X+C)}{3Y} \quad (22)$$

The probability of a collision between a particle and a bubble is given by^(3,4) (Equation 23)

$$P_c = \frac{2 u_b D}{9(u_b + u) Y} \left(\frac{d}{d_b} \right)^2 \left[\sqrt{(X+C)^2 + 3Y^2} + 2(X+C) \right]^2 \quad (23)$$

The collision is followed by attachment and if P_a denotes the probability of attachment then the probability of a successful sequence of collision and attachment would be $P = P_c P_a$. As in the case of Rogler⁽³⁾ and Rogler, Heaslip and Mehrvar,⁽⁴⁾ it is assumed, that the process is controlled by collision, namely $P \sim P_c$. Now, if n is the number of inclusions per unit volume of liquid the rate of inclusion removal by bubbling is given by (Figure 7) (Equations 24 and 25):

$$\frac{dn}{dt} = -K n \quad (24)$$

or

$$n_e = n_o e^{-K t} \quad (25)$$

Here n_o and n_e are the number (per unit volume) of inclusions at the entry of the bubbling zone and at the exit of bubbling zone respectively, t is the liquid average residence time inside the bubbling zone; t can be estimated as a fraction of liquid residence time inside the tundish (Equation 26),

$$t = \tau \frac{L}{L_T} \quad (26)$$

(relevant data for calculating τ are: tundish capacity, 320 liters and volumetric flow rate, 100 Lpm of water). K , the rate constant for the removal process can be estimated as follows. First the number of collecting collisions (collisions followed by attachment), N_{cc} , inside the volume of influence of each bubble is given by (the geometrical parameters L_T , L and H as defined in Figure 7) (Equation 27):

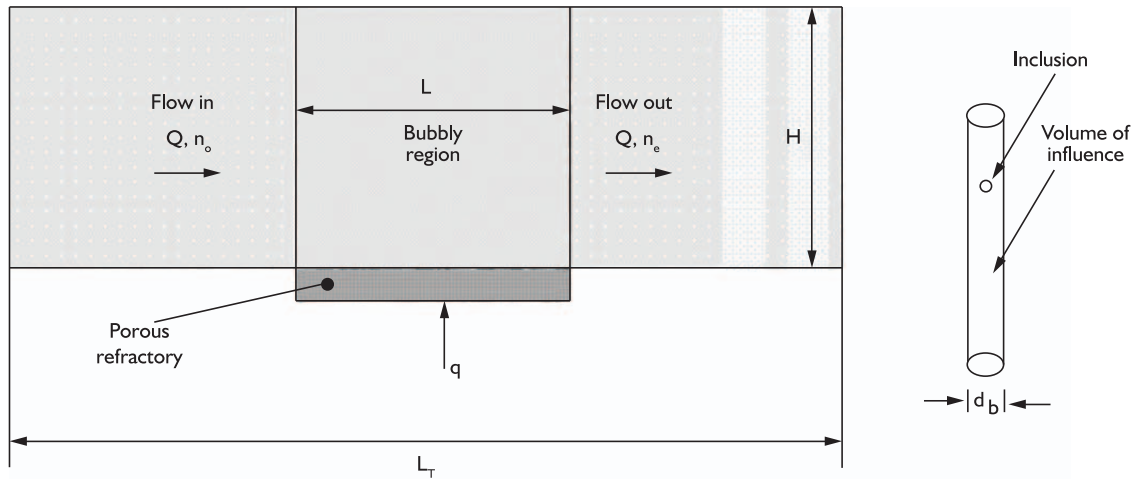


Figure 7. Schematics for bubbling inclusion flotation.

$$N_{cc} = \left(\frac{\pi}{4} d_b^2 H \right) n P \quad (27)$$

The number of bubbles supplied to the liquid, per unit time and unit of bubbling zone, N_b , is given by (Equation 28):

$$N_b = \frac{q}{(\pi d_b^3 / 6)} / (V_T L / L_T) \quad (28)$$

Here H is the level of liquid inside the tundish (0.43 m); q is the volumetric gas flow rate (corresponding to 0 to 10 Lpm of air); V_T is half of the tundish capacity (0.160 m³); L_T is the tundish half length (1.4 m); L is the length of the bubbling zone (0.15 m). Thus the number of collecting collisions per unit volume of bubbling zone would be (Equation 29):

$$N_T = N_{cc} \cdot N_b = \left(\frac{\pi}{4} d_b^2 H \right) n P \frac{q}{(\pi d_b^3 / 6)} / (V_T L / L_T) = K n \quad (29)$$

where the inclusion removal constant is (Equation 30):

$$K = \left(\frac{3}{2} H \right) P \frac{q}{d_b} / (V_T L / L_T) = \frac{3}{2} P \frac{q}{d_b A_b} \quad (30)$$

Here A_b is the area of the bubbling element. The efficiency of inclusion removal (by bubbling) can be defined as (Equation 31)

$$\varepsilon = \frac{n_o - n_e}{n_o} = 1 - e^{-K t} \quad (31)$$

Figure 8 gives the results of variation of efficiency of removal of inclusions with bubble size and inclusion size calculated for the present case.

It can be noticed that there is a strong influence of the bubble size. This effect can be made apparent by comparison of the data for basic and aluminate refractory bubbling elements, represented in Figure 4. The relationship of efficiency of inclusion removal as a function of gas flow rate is almost linear for larger bubble sizes. For larger inclusion sizes, the likelihood of collisions is higher. This results in better efficiency of removal due to bubbles, (Figure 4). However this model does not account for the influence of the length of the bubbling element on the removal efficiency as shown in these experiments. According to this model the rate constant of inclusion removal, K , increases for shorter bubbling elements, whereas the residence time of liquid inside the bubbling zone (t) decreases. Also the effect of position of the bubbling element on the inclusion removal efficiency is not accounted for.

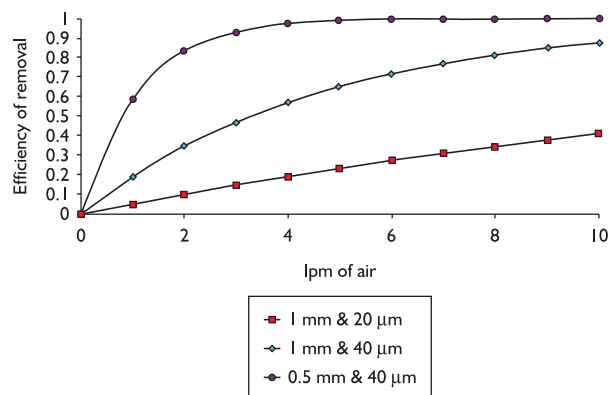


Figure 8. Effect of bubble size (mm) and inclusion size (μm) on the efficiency of removal, as calculated with the proposed tundish model.

However the orders of magnitude of experimental results and those predicted by this model seem to be in good agreement. Hence the model can be used as a reasonable tool to analyze and improve the industrial system.

5 CONCLUSIONS

Under the experimental conditions investigated with the physical model, the following observations and conclusions can be made:

- 1) The gas curtain acts as a filter or barrier and promotes an upward flow of liquid favouring separation and removal of inclusions. This effect is more pronounced with the increased proximity of the gas curtain to the ceramic nozzle.
- 2) For all combinations of flow, position and dimensions of the porous plug, a reduction of the piston flow fraction resulted in comparison to a tundish without gas injection system.

- 3) Larger porous plug sizes and larger particle sizes resulted in better flotation and separation;
- 4) Basic porous blocks seem to be more effective than the acid ones. The reason can be attributed to the pore structure and consequent resulting size of bubbles.
- 5) Bubbling of gas around the strand is also beneficial to the inclusion removal. However the efficiency is 25% lower than the one obtained with the porous block.
- 6) The results of the proposed simplified mathematical model for inclusion removal by bubbling are in reasonable conformity with the experimental results.

Acknowledgements

The authors wish to thank and acknowledge partial funding by FAPEMIG, CNPq and ArcelorMittal, Brazil.

REFERENCES

- 1 ZHANG, L.; THOMAS, B. G. State of the art in the control of inclusions during steel ingot casting. *Metallurgical and Materials Transactions B*, v. 37, n. 5, p. 733-61, 2006. <http://dx.doi.org/10.1007/s11663-006-0057-0>
- 2 MIKI, Y.; THOMAS, B. G. Modelling of inclusion removal in the tundish *Metallurgical Transactions B*, v. 30, n. 4, p. 639-54, 1999.
- 3 ROGLER, J. P. *Modelling of inclusion removal in a tundish by gas bubbling* MAS. 2004. 80 p. Thesis (Master of Applied Science) – Ryerson University, Toronto, Canada 2004
- 4 ROGLER, J. P.; HEASLIP, L. J.; MEHRVAR, M. Inclusion removal in a tundish by gas bubbling. *Canadian Metallurgical Quarterly*, v. 43, n. 3, p. 407-16, 2004.
- 5 THOMAS, B. G.; BAI, H. Nozzle clogging tundish: application of computational models. In: PROCESS TECHNOLOGY DIVISION CONFERENCE PROCEEDINGS, 18., 2001, Baltimore, MD. *Proceedings...* Warrendale, PA: Iron and Steel Society, p. 895-912.
- 6 ZHANG, L.; PLUSCHKELL, W.; THOMAS, B. G. Nucleation and growth of Alumina inclusions during deoxidation of steel. In: STEELMAKING CONFERENCE, 85., Nashville, 2002. *Proceedings...* Warredale: Iron and Steel Society, 2002. p. 463-76.
- 7 WANG, L.; LEE, H. G.; HAYES, H. A new approach to molten steel refining using fine gas bubbles. *ISIJ International*, v. 36, n. 1, p. 17-24, 1996. <http://dx.doi.org/10.2355/isijinternational.36.17>
- 8 WANG, L.; LEE, H. G.; HAYES, H. Prediction of optimum bubble size for inclusion removal from molten steel by flotation. *ISIJ International*, v. 36, n. 1, p. 7-16, 1996. <http://dx.doi.org/10.2355/isijinternational.36.7>

Recebido em: 23/08/2011

Aceito em: 19/12/2011